



SURVEYING THREE-DIMENSIONAL PERSPECTIVES OF THE FLOW STRUCTURE AROUND THE BRIDGE PILE DEPENDING ON THE VEGETATION PATTERN DISTRIBUTION

NAZANIN MOHAMMADZADE MIYAB¹, RAMIN FAZLOULA^{2*} ,
MANOUCHEHR HEIDARPOUR³, ATAOLLAH KAVIAN⁴ ,
JESÚS RODRIGO-COMINO⁵ 

¹*Ph.D. Graduated, Water Engineering Department, Sari Agricultural Sciences and Natural Resources University, Sari, Iran.*

²*Water Engineering Department, Sari Agricultural Sciences and Natural Resources University, Sari, Iran.*

³*Water Engineering Department, Faculty of Agriculture, Isfahan University of Technology, Isfahan, Iran.*

⁴*Watershed Management Department, Sari Agricultural Sciences and Natural Resources University, Sari, Iran.*

⁵*Department of Regional Geographic Analysis and Physical Geography, Faculty of Philosophy and Letters, Campus Universitario de Cartuja, University of Granada, 18071 Granada, Spain.*

ABSTRACT. Modeling techniques have enabled us to understand how to protect vital infrastructures using nature-based solutions. In this research, we demonstrated that by selecting a specific vegetation pattern distribution upstream of the pile as a nature-based solution, we could reduce the amount of scouring around the bridge piles. This is essential to avoid the negative impacts that occur after landslides, flash floods, or mudflows close to populated areas. This solution can mitigate the global problem of bridge failure. To achieve this goal, an Acoustic Doppler Velocimetry device (ADV) was used to measure the velocity components in an experimental channel with a 90 cm width, 15 meters long, and 60 cm high. Two different widths of vegetation were used: the overall vegetation, with a 90 cm width, and the patched one, with a 10 cm width, positioned upstream of the bridge pile. In the case of using patched vegetation, a 36% reduction was observed in the amount of scouring around the bridge pile compared to the free-vegetation case, showing the positive effect of using vegetation to reduce scouring. In both cases, the amount of negative Reynolds shear stresses decreased when the presence of vegetation was registered. Using octant analysis, the overall vegetation was shown to convert internal events into external ones in front of the pile. However, in the case of using patched vegetation, internal events were also observed in addition to external events. Patchy vegetation changed the transverse direction of outward vortices from internal to external. In the presence of patchy vegetation, the dominance of the inward event decreased sharply. The presence of vegetation in the flow path affected some bursting events and, as a result, reduced scouring. The results showed that each of the used vegetation models has a different effect on bursting events, and these events can affect the amount of scouring hole depth.

Estudio de las perspectivas tridimensionales de la estructura de flujo alrededor del pilote del puente en función de la distribución del patrón de vegetación

RESUMEN. Las técnicas de modelado nos permiten comprender cómo proteger infraestructuras vitales mediante soluciones basadas en la naturaleza. En esta investigación, demostramos que, al seleccionar una distribución

específica del patrón de vegetación aguas arriba de un pilote, podríamos reducir la cantidad de socavación alrededor de los pilotes de un puente. Esto es clave para evitar los impactos negativos que ocurren después de los deslizamientos de tierra, las inundaciones repentinas o los flujos de lodo cerca de áreas pobladas. Esta solución puede mitigar la desestabilización de infraestructuras como los puentes. Para lograr este objetivo, se utilizó un dispositivo de *Velocimetría Acoustic Doppler* (VAD) para medir los componentes de velocidad en un canal experimental de 90 cm de ancho, 15 metros de longitud y 60 cm de altura. Se utilizaron dos anchos diferentes de vegetación: la vegetación en general, con un ancho de 90 cm, y la parcheada, con un ancho de 10 cm, ubicada aguas arriba del pilote del puente. En el caso de usar vegetación parcheada, se observó una reducción del 36% en la cantidad de socavación alrededor del pilote del puente en comparación con la vegetación libre, mostrando el efecto positivo de utilizar vegetación para reducir la socavación. En ambos casos, la cantidad de tensión negativa de Reynolds disminuyó en presencia de vegetación. Mediante un análisis de octantes, se demostró que la vegetación en general convirtió los eventos internos en externos frente a la estructura. Sin embargo, en el caso de utilizar vegetación parcheada, también se observaron eventos internos además externos. En presencia de vegetación irregular cambió la dirección transversal de los vórtices hacia afuera de internos a externos. En presencia de vegetación irregular, la dominancia del evento interno disminuyó bruscamente. La vegetación en la trayectoria del flujo afectó algunos eventos de fractura y, como resultado, redujo la socavación. Los resultados mostraron que cada uno de los modelos de vegetación utilizados tiene un efecto diferente en los eventos de fractura y estos eventos pueden afectar la profundidad del agujero de socavación.

Keywords: Coherent structure, octant analysis, quadrant analysis, vegetation management, nature-based solutions.

Palabras clave: Estructura coherente, análisis de octantes, análisis de cuadrantes, gestión de la vegetación, soluciones basadas en la naturaleza.

Received: 20 June 2023

Accepted: 13 November 2023

***Corresponding author:** Ramin Fazloulou. Water Engineering Department, Sari Agricultural Sciences and Natural Resources University, Mazandaran province, Iran. E-mail: r.fazloulou@sanru.ac.ir; raminfazl@yahoo.com

1. Introduction

Scouring transfers materials from the bed and riverbanks around the bridge piles, abutments, and other hydraulic structures by the water flow (Shahriar *et al.*, 2021). It is important to note that three primary sources of scour contribute to the final results, which are: (i) long-term aggradation and degradation, (ii) contraction scour, and (iii) local scour. Long-term aggradation involves the deposition of material eroded from the upstream of the bridge. In contrast, degradation is scouring that occurs due to a deficit in sediment supply from upstream over relatively long reaches, as appearing in clear-water conditions (Arneson *et al.*, 2012). Several studies in the United States have reported extensive irreparable damages caused by bridge failure due to scour and state that scour around foundation structures is a leading cause of bridge collapse (Briaud *et al.* 2005). The defeat due to erosion and irreparable damages is not only an issue in the United States but globally. Considering the future scenarios where climate change could incorporate a concentration of extreme precipitation events after long periods of droughts, extreme weather conditions, and efficient solutions becoming indispensable (Clarke *et al.*, 2022). The potential economic, financial, and human life lost due to scour-induced failures signifies the importance of identifying the principal causes of scour and taking necessary mitigation actions before damage is incurred (Short *et al.*, 2016).

Many empirical models have been developed to estimate the equilibrium scour depth in bridge piers (Vonkeman and Basson, 2019). The development of these models includes experimental and field

data or both, ultimately leading to the creation of mathematical and numerical models (Shahriar *et al.*, 2021). However, scouring around the piers is a complex process influenced by many factors that are not considered when developing empirical models (Ettema *et al.*, 1998). Also, under the same hydraulic and geometric conditions, different models give significantly different scour estimates. In the design step, using a model that gives non-conservative results may lead to bridge failure, while choosing a very conservative model would lead to an unfavorable economic effect (Beg and Beg, 2013). This issue highlights the necessity of investigating the flow structure around the bridge foundation in different laboratory conditions and understanding and documenting foundation scouring estimation models after a comprehensive understanding of the flow structure.

In general, two approaches have been proposed to prevent the scouring of bridge piers. First, strengthening the bed, and second, changing the flow pattern to reduce the strength of the eddies created around the pile (Zaid *et al.*, 2019). To date, many results have been reported on the interaction between flow and vegetation in channels. For example, the effects of patched vegetation on river morphology, sediment transport, and hydro-environmental sequences have been demonstrated to be very efficient (Caroppi *et al.*, 2019; Afzalimehr *et al.*, 2021). Using vegetation as a nature-based solution would allow protecting rivers, controlling erosion, and trapping sediments (Rossi *et al.*, 2018). Vegetation in rivers and floodplains increases resistance, decreases flow capacity, and changes sediment transport and sedimentation (Mohammadzade *et al.*, 2015). The interaction between flow and vegetation is a complex process, and research in this field has led to essential simplifications in practical applications (Tempest *et al.*, 2015). Investigation of the flow velocity and turbulence intensity distribution around the bridge pile when vegetation is present in the scouring area could provide helpful information. It is well-known that vegetation absorbs significant momentum (Huai *et al.*, 2019), thereby changing the shear stress distribution structure, but this condition has yet to be examined around bridges.

According to past research (Miyab *et al.*, 2022), it can be predicted that the presence of vegetation upstream of the bridge pile can be an effective solution in reducing the amount of scouring. However, investigating the flow structure around the bridge pile is still unknown and has outstanding potential. Supposing the presence of vegetation can be a factor in protecting the bridge piles against the scouring phenomenon. In that case, it will be valuable to analyze its interaction with the flow around the bridge foundations based on studying turbulent flow components. In addition to being simple and cost-effective, the vegetation solution does not add to the construction costs. Although the studies conducted on the scouring of bridge foundations are extensive, they have yet to provide a single solution to reduce scouring for different hydraulic conditions, which indicates a weakness in understanding the structure and behavior of the flow around the bridge foundation. Also, most of the methods used in the studies are not environmentally friendly. Therefore, in the current research, the vegetation cover upstream at different spatial patterns will be evaluated as an effective solution to change the flow structure to reduce the eddies created around the bridge pile. This research desires to recognize the coherent flows formed around the bridge pile in the presence and absence of vegetation through quadrant and octant analysis. Furthermore, the amount of Reynolds shear stress and scour profile formed around the bridge support are investigated when vegetation is located upstream of the bridge pile.

This research aims to investigate the effect of different vegetation patterns upstream of bridge piles on flow structure, coherent flows, Reynolds shear stress, and scour profile. Specifically, it will compare the flow velocity and turbulence intensity distribution around bridge piles with and without vegetation and analyze the effect of different vegetation patterns on bursting events and scour depth. We consider this research significant in terms of multidisciplinary due to its diverse applications within control measures related to physical geography, forestry, civil, and terrain engineering studies. Vegetation cover is a simple, cost-effective, and environmentally friendly solution to reduce the loss of money invested in vital infrastructures. This study allows us to understand the flow structure around bridge piles with vegetation, which could be essential for designing effective protection measures for land management plans from the catchment to the regional scales.

2. Methods and Materials

2.1. Experimental channel

This study was conducted in a flume with a length of 15 meters, a width of 90 cm, and a height of 60 cm, featuring a maximum flow rate of 50 liters per second, located in the hydraulic laboratory of Isfahan University of Technology. The flume had a plexiglass bottom and sidewalls, presenting a rectangular cross-section. The water level was regulated by a sliding gate downstream of the flume. To mitigate turbulence in the flow, there was a flow-calming chamber in the inlet tank constructed with perforated bricks and honeycomb. A digital flow meter measured the flow rate of the inlet stream. Throughout the channel, excluding one meter at the beginning and end, a Teflon platform was installed, standing 20 cm high. A layer of sediments, composed of bed material, was affixed to the platforms to adjust the roughness coefficient. In each series of experiments, a one-meter distance between two platforms was filled with sifted sand, and its surface was smoothed entirely using a trowel and a leveler. Figure 1a shows the schematic view of the experimental channel.

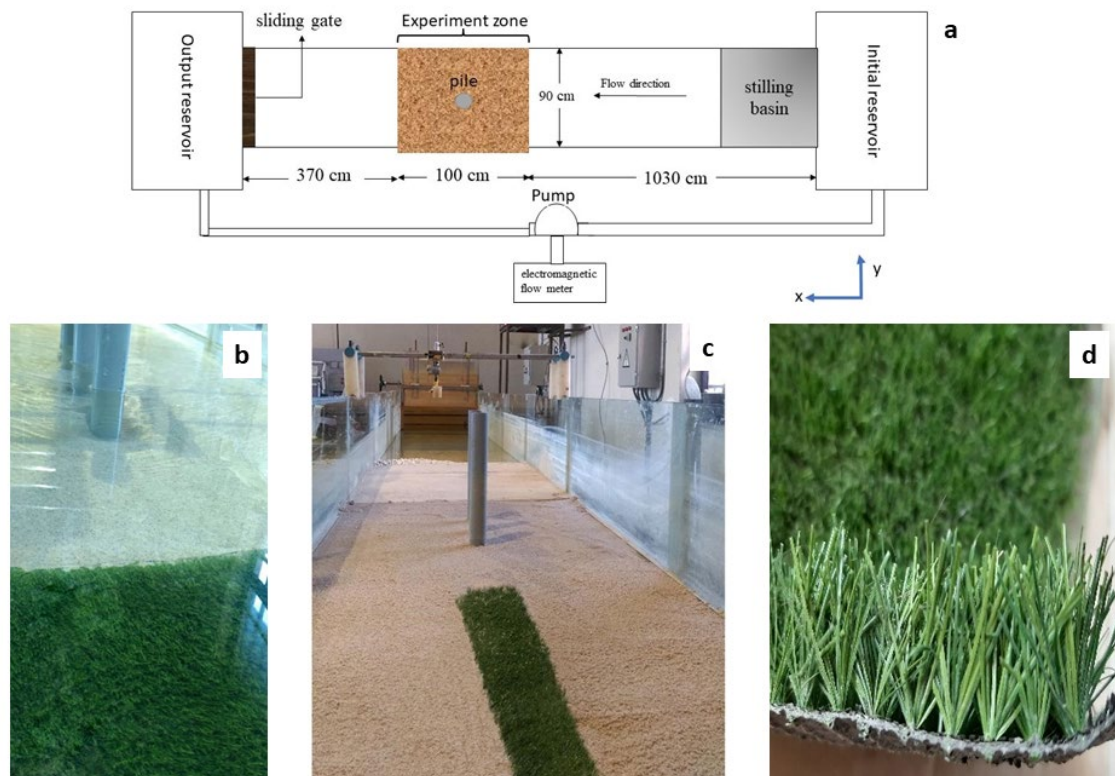


Figure 1. a) The schematic view of the experimental, b) the distribution of overall vegetation upstream of the bridge pile, c) the distribution of patch vegetation upstream of the bridge pile and figure d) the density of used vegetation channel.

2.2. Depth and velocity meters

A limnimeter with an accuracy of 1 mm was used to measure the scour hole profile. This limnimeter was placed on a frame with four support points on the upper edge of the channel. Two parallel bars were attached to the frame body for its transverse movement. In this way, the limnimeter could move in two directions perpendicular to each other and easily measure the scour profile (Kabiri *et al.*, 2022). Velocity measurement was conducted at different points using the new generation ADV three-dimensional velocity meter manufactured by Nortek, Norway. Due to the cable structure of this device, it was possible to measure the velocity from different angles. The manufacturer calibrated this device,

and it remains unchanged as long as the device is not physically damaged. This device can assess the characteristics of turbulence. One of the merits of this device is its ability to collect data with high frequency and measure far from the desired surface, minimizing the difference caused by the presence of the measuring device in the flow. Measurements in the ADV device are based on a physical phenomenon called the Doppler effect.

The number of raw data recorded by the device depends on the frequency set for the device and the measurement time. In this project, ADV was set to 200 Hz and 2 minutes, resulting in the average velocity of a point among $120 \times 200 = 24,000$ points. Additional data collection and filtering software used were Vectrino+, WinADV, and Excel. To filter the data for each point among the 24,000 collected velocities, inappropriate data (correlation < 70 and SNR < 15 or SNR < 5) were removed, and based on other data, the average speed was obtained (Nortek, 2004).

2.3. The bed material size and pile diameter

In this study, following Chiew and Melville (1987), the diameter of the pile was chosen to be 5 cm (symbol D). The distance between the axis of the pile and the wall was suitable because of the channel width. The bridge pile was installed at a distance of 1062 cm from the channel's beginning. According to Raudkivi and Ettema (1983), to achieve the maximum scouring depth, the formation of ripples should be prevented. For this purpose, the average size of sediment particles should be greater than 0.7 mm. Chiew and Melville (1987) acknowledged that when the ratio of the pile diameter to the average size of the particles is greater than 50, the effect of the particle size on the scour depth can be ignored. In this research, sand particles with a diameter greater than 0.7 mm will be selected. The characteristics of the bed material are as follows (Pope, 2000):

$$\sigma_g = \left(\frac{d_{84}}{d_{16}}\right)^{0.5} \tag{1}$$

$$Gr = \frac{1}{2} \left(\frac{d_{84}}{d_{50}} + \frac{d_{50}}{d_{16}}\right) \tag{2}$$

$$D_g = (d_{16} \cdot d_{84})^{0.5} \tag{3}$$

$$Cu = \frac{d_{60}}{d_{10}} \tag{4}$$

Where d_{50} represents the average size of sediment particles, Cu is the uniformity coefficient, Dg means the geometric mean size, σ_g corresponds to the standard geometric deviation and Gr registers the grading factor. According to the uniformity coefficient of Cu and d_{50} , the type of sand bed material was uniform (McGlinchey, 2009). Table 1 shows the geometric characteristics of sediment particles.

Table 1. Geometric characteristics of sediment particles used in this research.

d₅₀ (mm)	Cu	Dg	σg	Gr
0.77	1.133	0.763	1.075	1.075

The thickness of the bed was determined according to the maximum scour depth. For this purpose, an estimate of the maximum scour depth was first obtained. Laursen (1963) presented the relationship based on the pile diameter to calculate the maximum scour depth.

$$d_{sm} = 1.05D^{0.75} \tag{5}$$

Where D is the pile diameter in meters and d_{sm} is the maximum scour depth in meters. Therefore, with the help of the above relationship and the chosen diameter of 5 cm for the pile, the maximum scouring depth of 11 cm was obtained, so the height of the substrate particles chose 20 cm to ensure accuracy.

2.4. Experimental setup

Two types of dense artificial grass vegetation with a height of two centimeters (10 % of the flow depth) were located upstream of the bridge pile. The vegetation used width is once 90 cm, i.e., the entire width of the stream (V_o), and once 10 cm of the stream width (V_p) in the central axis of the channel. The vegetation cover was placed 30 cm above the bridge pile. Figure 1b shows the distribution of overall vegetation upstream of the bridge pile, Figure 1c shows the distribution of patch vegetation upstream of the bridge pile and Figure 1d shows the density of used vegetation. A single pile with a 5 cm diameter was placed perpendicular to the bed in the flow direction to conduct the experiments. The shields diagram was used to determine the appropriate hydraulic conditions for maximum scour (Cao *et al.*, 2006). An average flow rate of 0.036 m³/s and a depth of 20 cm were established for the channel's sand bed. At the experiment's end, the scour hole dimensions were measured. Eventually, several velocity profiles were taken using ADV upstream and downstream of the bridge pile.

2.5. Reynolds shear stress (RSS)

Reynolds shear stress (RSS) is a measure of the friction between layers of a fluid due to turbulent flow. It is a key factor in sediment transport and other physical processes. RSS is caused by the uneven motion of fluid particles in turbulent flow. When fluid particles collide with each other, they transfer momentum from one particle to another. This transfer of momentum creates friction between the layers of fluid. RSS is important in physical geography and civil and terrain engineering studies because it plays a role in various physical processes, such as sediment transport, erosion, and deposition. For example, RSS can erode riverbanks and transport sediment downstream. It can also cause the deposition of sediment in floodplains and estuaries. RSS is also crucial for understanding river flow and other fluid dynamics. Turbulent currents account for a significant part of river flows. In this flow type, fluid particles deviate from their original path and move irregularly. In this case, in addition to the fluid's inherent viscosity, the dispersed movements of particles also contribute to flow resistance, and a feature called eddy viscosity is introduced to express it (Pickering *et al.*, 2021).

Turbulent flow characteristics play a significant role in the sediment transport process, including diffusion, erosion, sedimentation, and flow resistance. In turbulent flow, the generation and destruction of small and large eddies cause fluctuations in flow parameters. In this flow, instantaneous parameters such as velocity can be expressed as follows:

$$u = \bar{u} + u' \quad (6)$$

$$v = \bar{v} + v' \quad (7)$$

$$w = \bar{w} + w' \quad (8)$$

Where \bar{u} , \bar{v} and \bar{w} are the time average of the velocity components in x, y and z directions and u' , v' and w' are the fluctuation values of velocity.

Reynolds shear stress is calculated from the following equation:

$$\tau = -\rho u'w' \quad (9)$$

2.6. Quadrant analysis

Turbulent flow in open channels is not a completely random process. However, some continuous temporal and spatial patterns can be identified in them. These patterns are known as coherent structures in turbulent flow. They significantly affect the distribution of shear stress in open channel processes. As a result, coherent structures play an essential role in the erosion and sedimentation of the bed, the phenomena of mixing, nutrient distribution in the river, and aquatic plant implantation. Coherent structure in flow refers to a three-dimensional region of the flow in which at least one of the main

variables of the flow (for example, velocity, temperature, and density components) shows a significant correlation with itself and with another variable in a range of time and space. This temporal and spatial spectrum is much larger than the flow's most minor local temporal and spatial scales (Cellino and Lemmin, 1999).

Turbulence has a significant inherent complexity, leading to various interpretations of its nature. The quadrant analysis method is used to study the presence of coherent structures in flow fields and their contribution to the total shear stress. The quadrant analysis method involves studying the relationship between the velocity fluctuations in the flow direction (u') and perpendicular to the flow (w'). For this, u' and w' are plotted against each other, forming a quadrant plane in the trigonometric coordinate system, as indicated in Table 2. This plane represents a bursting cycle (Carino and Brodkey, 1969; Lu and Willmarth, 1973; Willmarth and Lu, 1972), including the four events.

Table 2. A quadrant plane in the trigonometric coordinate system.

Bursting name	Quadrant	u'	w'	Property
Outward	Q1	+	+	High speed fluid away from the bottom
Ejection	Q2	-	+	Low speed fluid away from the bottom
Inward	Q3	-	-	Low speed fluid moving to the bottom
Sweep	Q4	+	-	High speed fluid moving to the bottom

The occurrence probability of event k is calculated as the normalized occurrence frequency, f_k , for a particular class of events related to different classes of events (Termini, 2015):

$$f_k = \frac{n_k}{N} \tag{10}$$

$$N = \sum_1^4 n_k \quad k = 1, 2, \dots, 4$$

Primary research to understand the turbulent structure of coherent flows in channel walls and beds dates back to the last 30 years (Corino and Brodkey, 1969; Kline *et al.*, 1967; Kim *et al.*, 1971; Grass 1971; Afzalimehr and Anctil, 2000). Some researchers interpreted this coherent structure as periodically organized events in the time domain that manifest their impact in the Reynolds shear stress time series (Carino and Brodkey, 1969; Lu and Willmarth, 1973). The first event (Q_1) involves the occurrence of high-velocity fluid movement from the bed to the water surface, the second event (Q_2) is characterized by low-velocity fluid movement to the water surface, the third event (Q_3) involves low-velocity fluid movement toward the bed, and the fourth (Q_4) event shows high-velocity fluid movement towards the bed. The cycle that includes these four events is referred to as bursting events (Kabiri *et al.*, 2022). It is important to note that ejection and sweep events generate turbulent energy, and outward and inward interactions are associated with energy dissipation. Additionally, ejection and sweep are often linked to the removal and transfer of sediments (Pope, 2000; Vijayasree *et al.*, 2020). Sweep events are associated with the initiation of bed load movement, while ejections are responsible for lifting and carrying the bed load (Sterk *et al.*, 1998). The investigation of the flow downstream of the submerged vegetation patch by Mayaud *et al.* (2016) demonstrated high frequencies of Q_2 (ejection) and Q_4 (sweep) events in the crest of the vegetation patch (Mayaud *et al.*, 2016). In contrast, it is reported that the dominance of outward and inward interactions in the shear layer is induced by the flow passing above the vegetation patch, which is a notable characteristic of the flow in the downstream region of a submerged vegetation patch in a more distant region (Kazem *et al.*, 2021a; Przyborowski *et al.*, 2019; Keshavarzi *et al.*, 2014).

2.7. Octant analysis

As mentioned, quadrant analysis is based on the analysis of the probability distribution of the two longitudinal (u') and vertical components (v') of the velocity fluctuation. However, in rivers and natural channels, the flow structure is coherently structured in three dimensions, especially where an obstacle is placed in the flow path. The velocity in the lateral direction cannot be neglected, as it can induce significant secondary circulation (Keshavarzi *et al.*, 2014). Additionally, two-dimensional analysis cannot define sediment entrainment as a three-dimensional phenomenon (Ortiz *et al.*, 2013; Zong and Nepf, 2010). In general, eight burst event classes in 3D octant analysis are defined based on the sign of velocity fluctuations, as outlined in Table 3. The symbols used in this research are inspired by the work of Keshavarzi *et al.* (2014) and Kazem *et al.* (2021b). Keshavarzi (2014) stated that the deviations of group events are towards the internal direction or the central line (internal events), while the deviations of group B events are away from the central line and towards the channel walls (external events) (Keshavarzi *et al.*, 2014). This study considers three categories of results for octant analysis: (1) the probability of occurrence of bursting events (Op), (2) the attack angle of bursting events, and (3) the stability of each event (S_i). Calculating the probability of occurrence of events is similar to the quadrant analysis approach. It is equal to the frequency of occurrence (f_k) for a specific event class relative to different events (Bento *et al.*, 2021).

$$f_k = \frac{n_k}{N} \quad (11)$$

$$N = \sum_{k=1}^8 n_k, k = 1, 2, 3, \dots, 8$$

Table 3. Eight bursting event classes in 3D octant analysis based on the sign of velocity fluctuations.

Group	Classes of Bursting Events	Class name	u'	v'	w'
A (internal)	Outward interaction	PPP	+	+	+
	Ejection	NNP	-	-	+
	Inward interaction	NNN	-	-	-
	Sweep	PPN	+	+	-
	Outward interaction	PNP	+	-	+
B (external)	Ejection	NPP	-	+	+
	Inward interaction	NPN	-	+	-
	Sweep	PNN	+	-	-

Octant analysis is a method for classifying bursts of turbulence in three dimensions, offering more detail than quadrant analysis, which only considers two dimensions. Turbulent bursts are sudden, localized increases in turbulence intensity and play a crucial role in sediment transport and other physical processes. The probability of occurrence of a burst is the fraction of time that the burst occurs at a given point in the flow field. The attack angle of a burst is the angle between the mean flow direction and the direction of the burst. The stability of a burst is a measure of how long the burst lasts. Table 3 displays the eight bursting event classes in 3D octant analysis based on the sign of velocity fluctuations. In this table, the symbol N is used for velocity fluctuations with a negative value, and P is used for positive velocity fluctuations in the class name column. The first letter represents u' , the second letter represents v' , and the third letter represents w' . The force applied to sediment particles in the bed strongly depends on the angle of inclination of the three-dimensional flow velocity fluctuations (θ_i). Understanding the attack angle of bursting events helps comprehend the entrainment sediment process (Breusers *et al.*, 1977; Bridge and Bennett 1992; Esfahani and Keshavarzi, 2011; Esfahani and Keshavarzi, 2013; Bernard and Handler, 1990). The attack angle is calculated as follows:

$$\theta_i = \left| \arctan \left(\frac{w'}{\sqrt{u'^2 - v'^2}} \right) \right| \quad (12)$$

Esfahani and Keshavarzi (2013, 2021) and Liu and Bai (2013) employed the aforementioned technique to comprehend the bursting process in a meandering channel (Liu and Bai, 2013; Carnacina *et al.*, 2019; Guan *et al.*, 2019). They recognized that this technique offers greater clarity in understanding coherent flow structures and their impact on sediment entrainment in meanders. Keshavarzi (2014) delved into the coherent structures around the bridge pile (Keshavarzi *et al.*, 2014). Their findings indicated that near the bed, internal ejection and external sweep events play a role in the scouring mechanism around the single bridge pile. Using this technique, Kazem *et al.* (2021b) examined the eddy structures in a channel with patched vegetation (i.e., artificial bars). They observed that in a channel with a small width of vegetation patch, the flow passing through the vegetation (x direction) and the side flow around the vegetation patch significantly influence the formation of flow structures outside the vegetation (Kazem *et al.*, 2021b). MATLAB programming software was employed for quadrant and octant analysis, and subsequent results were analyzed.

3. Results and discussion

3.1. Scouring contour map

Figure 2 (2a-2c) displays contour maps of scouring profiles for single piles without vegetation, with overall vegetation, and with patch vegetation, respectively. In all figures, the X-axis represents the distance from the beginning of the channel, and the flow direction is from left to right. Scouring depths are 6.5 cm in the free-vegetation case, 4.7 cm in the overall vegetation case (Vo-case), and 4.1 cm in the patchy vegetation case (Vp-case). According to the results of this research, the highest amount of scouring occurred in the free-vegetation case. Patched vegetation could reduce the scour depth by 36%. Additionally, vegetation decreased the longitudinal and transverse expansion of the scouring hole.

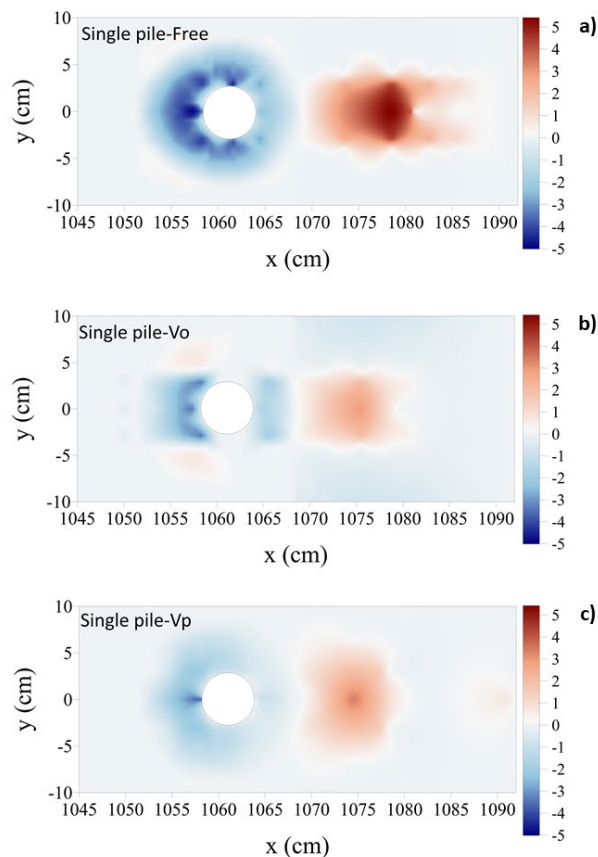


Figure 2. Contour map of scour profile for single pile a) in without vegetation case, b) in the presence of overall vegetation case and c) in the presence of patched vegetation case.

3.2. Reynolds shear stress

Figure 3 illustrates the distribution of Reynolds shear stress (RSS). The horizontal axis (x) indicates the distance from the beginning of the channel in centimeters, and the vertical axis (z) indicates the height from the bed represented in centimeters too. Given that RSS is proportional to the flow's capacity to transport sediments and reflects the exchange of turbulent motion between fluid layers, it is understandable that such capacity increases with the enlargement of the scour hole (Bernard Handler, 1990; Carnacina *et al.*, 2019). In all cases upstream of the pile, the region with the maximum RSS developed upstream of the scour hole. This is where the maximum flow power for scouring (area of large value enlarged) was established, aligning with the findings of Bento *et al.* (2021) and Guan *et al.* (2019). The maximum RSS occurs upstream of the pile where the maximum positive and negative velocity values occur, indicating that the velocity in this region can be highly unstable.

The presence of vegetation decreased the negative values of shear stress and reduced the intensity of RSS upstream of the pile. Downstream of the bridge pile, the negative values of shear stress increased, especially at the point closest to the pile, where these negative values are higher in the Vo-case. In the Vo-case, the highest shear stress values downstream of the pile occurred where the accumulation of sediments was observed.

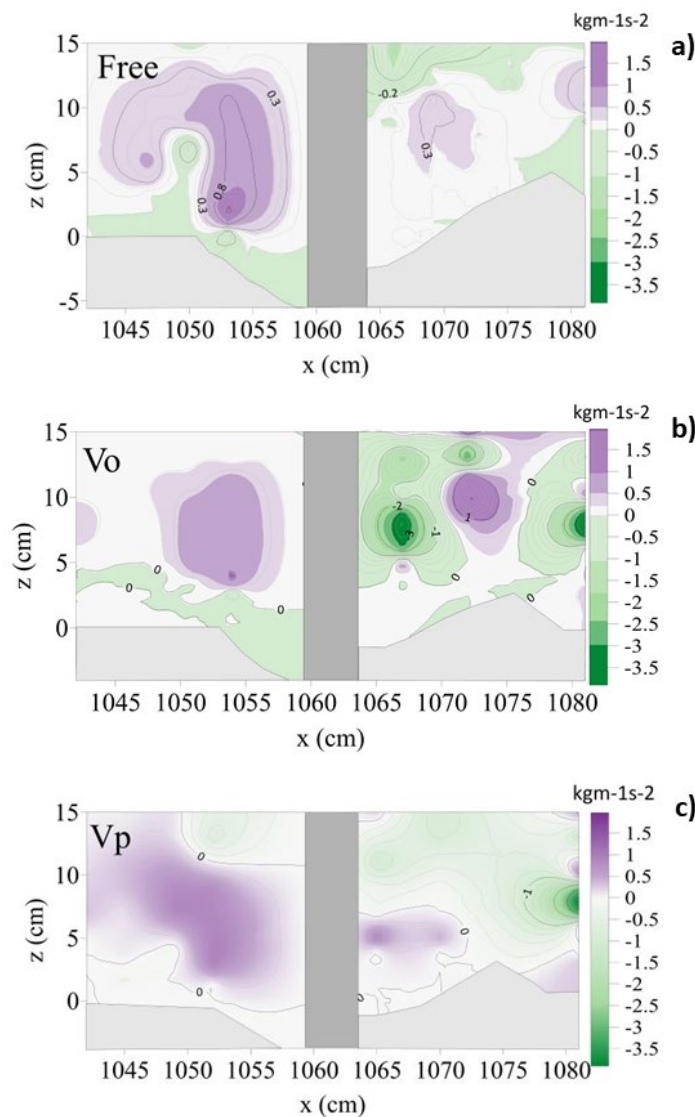


Figure 3. Reynolds shear stress distribution profile for single pile a) in without vegetation case, b) in the presence of overall vegetation case and c) in the presence of patched vegetation case.

3.3. Quadrant analysis

Figure 4 depicts the occurrence probability of quadrant classes. The location of the bridge pile is from $x=1059.5$ cm to $x=1064.5$ cm. The results demonstrated that in the upstream of the pile in the free-vegetation case, the sweep near the bed and the inward in the middle part of the flow depth were the dominant events, both of which increased as they approached the pile. The presence of vegetation caused a significant increase in the probability of ejection events at points very close to the bed and near the water surface and the sweep events at mid-depth points and near the bed. Kabiri (2022) also observed an increase in the probability of ejection and sweep in the presence of vegetation, which can be caused by a decrease in momentum of the water flow. In the free-vegetation case, the possibility of ejection and outward events is dominant downstream of the pile. In the presence of vegetation, the probability of an outward event increased in the middle flow depth range and was closer to the bed. Also, the ejection increased in the Vo-case near the water surface and in the Vp-case in the mid-depth of flow. In the upstream of the pile, the zone of ejection events in the Vp-case is closer to the water level than Vo-case, which is in accordance with Kazem et al.'s results (2021b). Downstream of the pile in the Vp-case, the ejection and sweep events are closer to the water surface and the outward and inward are closer to the bed. Also, the possibility of outward and inward occurrences has increased. The horizontal axes show x (cm), and the vertical axes show z (cm).

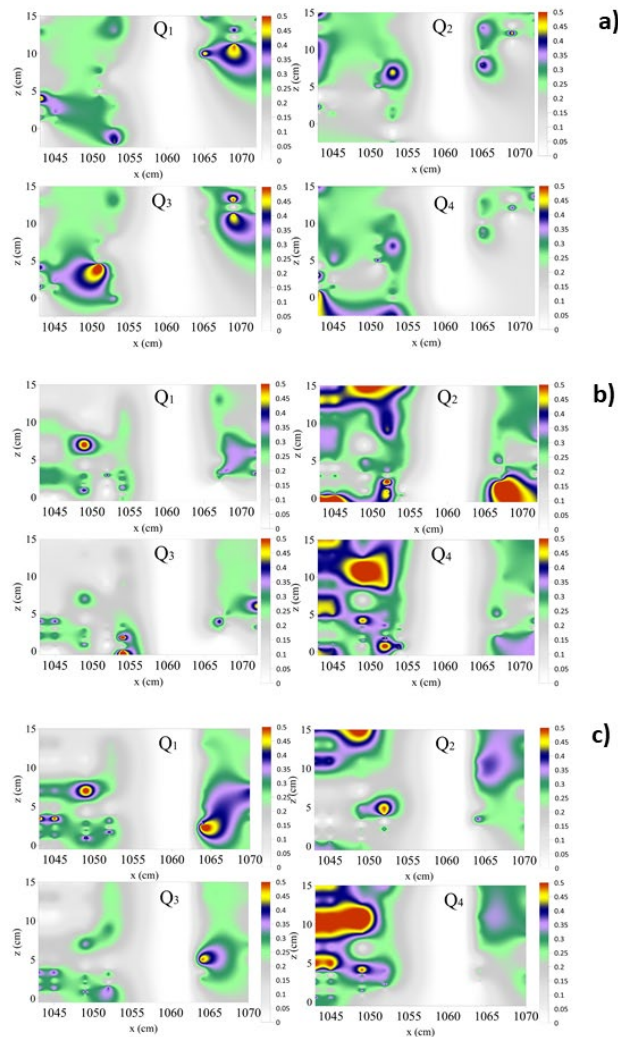
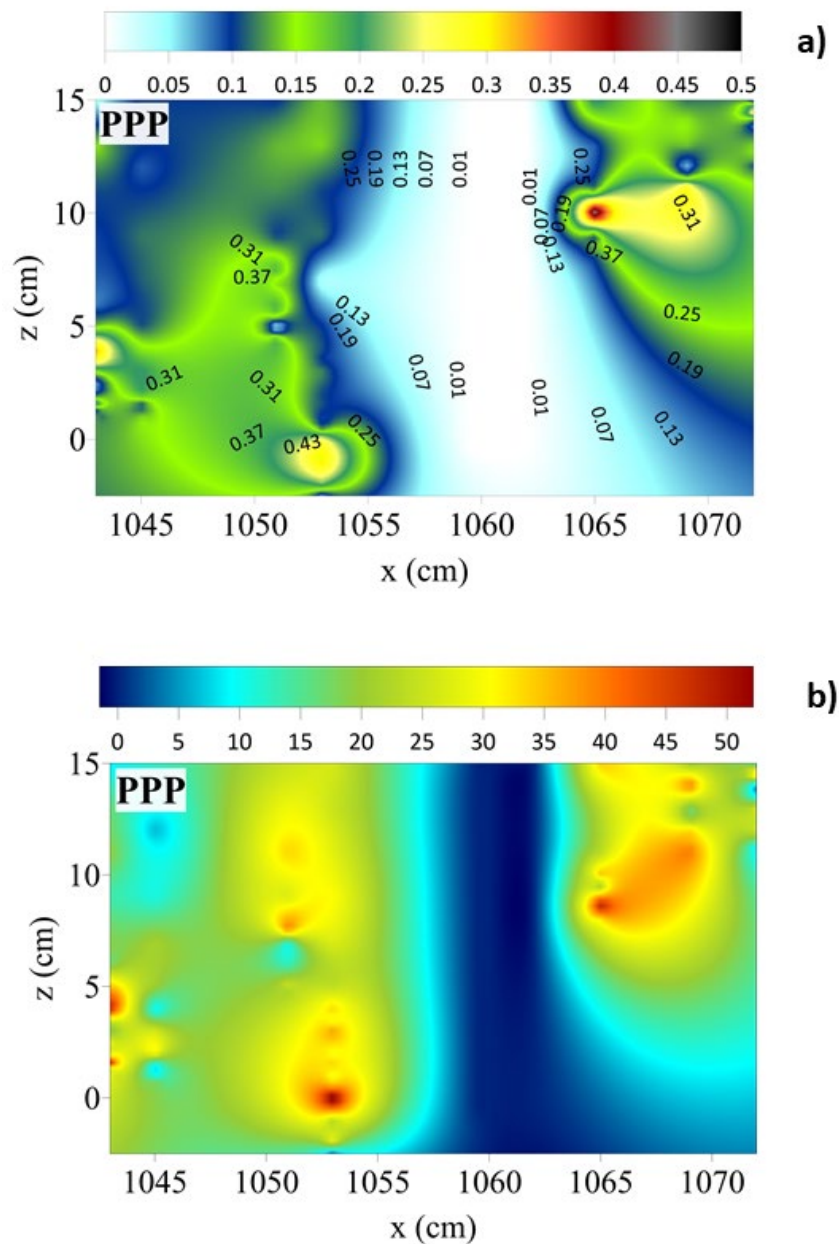


Figure 4. Probability of occurrence of quadrant classes profile for single pile a) in without vegetation case, b) in the presence of overall vegetation case and c) in the presence of patched vegetation case.

3.4. Octant analysis

Figure 5 illustrates the results of the O_p (probability of occurrence) of a sample of octant analysis events in the free-vegetation case, along with the S_t values for these events. The numbers inside the graphs indicate the angle of each event in radians. For better analysis, the flow depth was divided into three parts: the first zone, $z < 5$ cm (with two sub-zones, $z < 0$ cm and $0 < z < 5$ cm), the second zone, with $5 \text{ cm} < z < 10$ cm, and the third zone with $z > 10$ cm. In the free-vegetation case upstream of the pile: in the first zone of A's class, internal and outward occurrences (in sub-zone $z < 0$) have a 33% O_p and S_t of 57, and the angle of attack is close to 1 radian. In class B, external inward occurrences (in sub-zone $0 < z < 5$) with 42% O_p and 45 St are the most dominant phenomena, followed by internal ejection with 31% O_p and St of 49. In terms of stability, the events of internal outward, internal ejection, and external sweep near the bed have the highest values, consistent with the results of Keshavarzi *et al.* (2014).



In classes A and B of the second zone, the O_p of events was between 18 and 26 % (26% belonging to internal sweep), showing no dominant event. However, in terms of stability, internal ejection with 46 and internal sweep events with 45.3 was the most stable. In the third zone, the O_p varied between 15 and 24% (24 % belonging to internal ejection), and the S_t varied between 30 and 40%. Sediment scoured from the upstream accumulated behind the pile, creating a mound of sediment that caused Zone 1 to be absent. In the second zone downstream of the pile, external ejection is dominant, with a 30% O_p and S_t of 58 near the mound of sediments. Also, above that, internal outward is the most dominant event with a 47% O_p and S_t of 50. In the third zone near the water surface, internal inward, with a 47% O_p and S_t of 50, and external ejection, with a 43% O_p and S_t of 47, are the dominant events near the second zone. Angles of attack downstream of the pile are reduced compared to the upstream.

Figure 6 shows the results of the O_p of octant analysis event sample, and the S_t 's value of each octant event of Group B in the free-vegetation case. The numbers written inside the graphs show the angle of each event in radians. In the Vo-case at the pile upstream: in $z > 0$ cm, the dominant events are external ejection with a 60 % O_p and 57 % S_t and external inward with a 52 % O_p and 55 of S_t , and in $z < 0$ cm internal outward with 41 % O_p and S_t 57 is dominant. In the second zone, the O_p of events varied between 19 and 35 percent. In terms of stability, external outward with an O_p of 35 % and S_t of 57, followed by external sweep with an O_p of 34 % and S_t of 55, were the most dominant events. In the third zone, the external sweep is with an O_p of 52 % and S_t of 61, and in the second place is external ejection with an O_p of 30 % and S_t of 41.

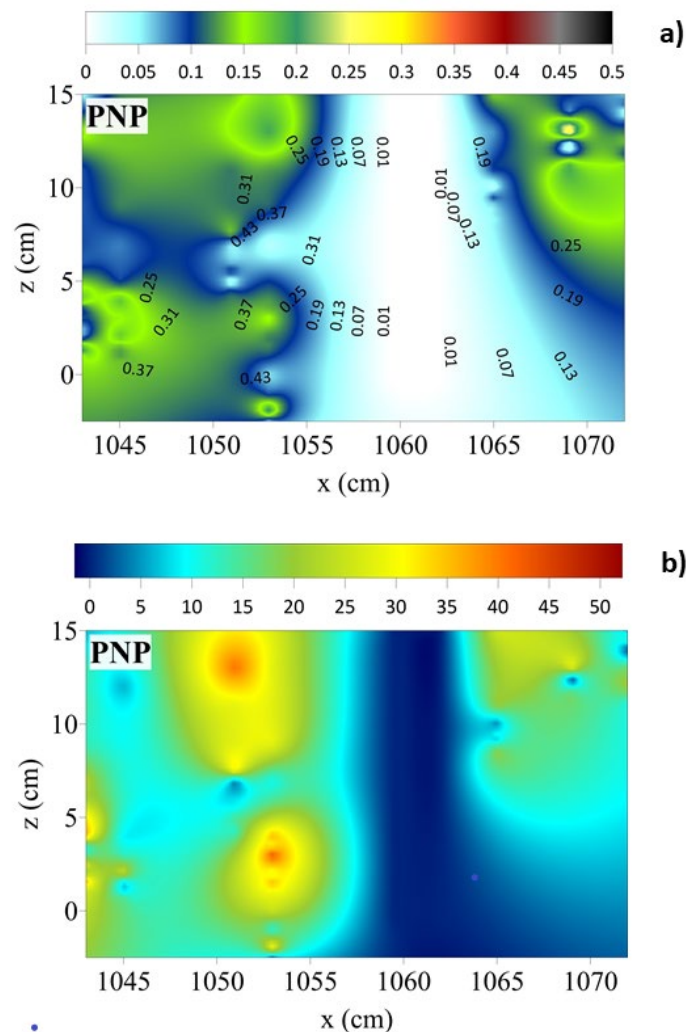


Figure 6. The sample of B group events of octant analysis: a) the O_p results; b) the S_t in free vegetation case.

Downstream of the pile in the first zone, external ejection was the most dominant event with O_p of 63 % and S_t of 45 %, followed by internal outward with a 33 % O_p and S_t of 56 %. In the second zone, internal outward with an O_p of 31 %, S_t of 52 % after that, internal ejection with an O_p of 29 %, and S_t of 41 % are the dominant events. In the third zone, the range of O_p was observed between 13 and 20 percent, showing no dominant phenomenon in this zone. In terms of S_t , external sweep had the highest stability, i.e., 42. Figure 7 shows the events of octant analysis: (a) the O_p results; (b) the S_t in Vo-case. Upstream of the bridge pile in the Vp-case: in the first zone, internal outward with a 61% O_p and 42 S_t , external sweep with a 39% O_p and 42 S_t , and internal ejection with 36% O_p and 65 S_t were the most dominant events. In the second zone, external sweep with O_p of 45% and S_t of 59, internal ejection with a probability of 36% and stability of 65 %, and external outward with an O_p of 35% and S_t of 57% were the dominant events. In the third zone, the external sweep was dominant with an O_p of 52% and S_t of 62 events.

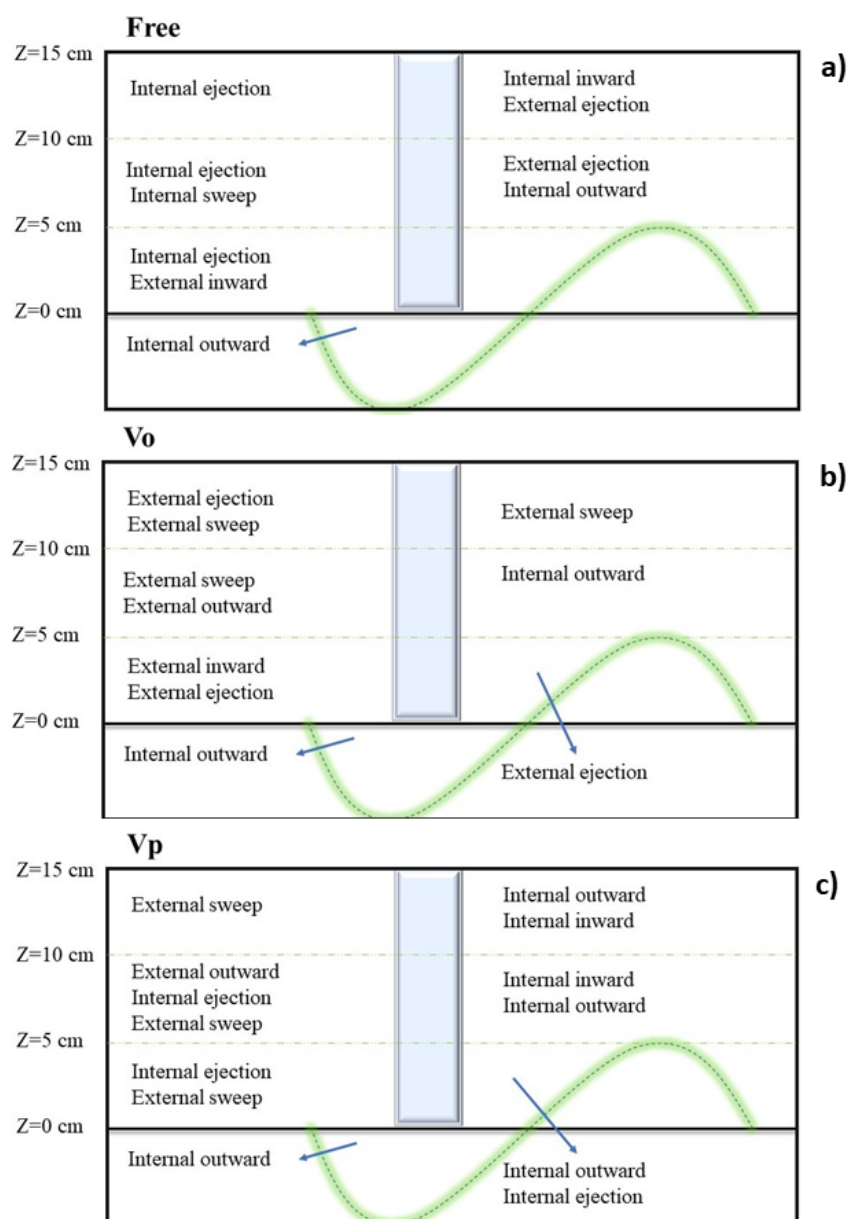


Figure 7. Schematic diagram of dominant phenomena upstream and downstream of the bridge pile a) in without vegetation case, b) in the presence of overall vegetation case and c) in the presence of patched vegetation case.

Downstream of the bridge pile in the Vp-case: in the first zone, internal outward with 47 % O_p and 52 S_t and internal ejection with 37 % O_p and 50 S_t were the most dominant events. In the second zone, internal inward with O_p of 37 % and S_t of 50 and internal outward with O_p of 31 % and S_t of 51 were the dominant phenomena. In the third zone, the O_p was between 9 and 26 percent, which internal outward having the most dominance with a 26 % O_p and 61 S_t . In terms of stability, internal inward has a S_t of 60 with an O_p of 18. Figure 7 schematically shows the bridge's pile, which phenomenon prevails in each zone.

4. Conclusions

This study highlights the substantial impact of vegetation on scour rate, Reynolds stress, and coherent flow structure around bridge piles. The presence of vegetation results in a remarkable 36% reduction in scour depth and induces changes in the distribution of Reynolds stress. The maximum Reynolds stress region shifts upstream of the pile, leading to a decrease in negative shear stress upstream and an increase downstream. Quadrant analysis illustrates that vegetation promotes the occurrence of ejection and sweep events, while octant analysis indicates the dominance of internal outward events within the scour hole. In the free-vegetation case, near the bed, the eddies move toward the walls, but as one moves away from the bed, the eddies shift toward the central axis. The overall vegetation redirects the flow towards the walls in the base area, reducing scouring. Stability and event probability increase with the presence of vegetation. Overall vegetation transforms internal events into external ones in front of the pile. However, in the case of patched vegetation, both internal and external events are observed. With a potential 36% reduction in scour depth, vegetation can play a crucial role in mitigating flood risk and stabilizing bridge structures. Future research should delve into quantifying the effects of various vegetation patterns and densities on flow characteristics and scour development. The findings hold substantial implications for flood risk management. Vegetation emerges as a key player in reducing flow velocity and scour depth, thereby enhancing flood resilience and decreasing the risk of bridge failure due to erosion. Engineers can leverage this information to inform the design and maintenance of structures in flood-prone areas, considering vegetation management strategies to bolster flood resilience.

References

- Afzalimehr, H., Riazi, P., Jahadi, M., Singh, V.P., 2021. Effect of vegetation patches on flow structures and the estimation of friction factor. *ISH Journal of Hydraulic Engineering* 27(sup1), 390-400. <https://doi.org/10.1080/09715010.2019.1660920>
- Afzalimehr, H., Anctil, F., 2000. Accelerating shear velocity in gravel-bed channels. *Hydrological Sciences Journal* 45(1), 113-124. <https://doi.org/10.1080/02626660009492309>
- Arneson, L.A., Zevenbergen, L.W., Lagasse, P.F., Clopper, P.E., 2012. *Evaluating scour at bridges* (No. FHWA-HIF-12-003). National Highway Institute (US).
- Beg, M., Beg, S., 2013. Scour reduction around bridge piers: A review. *International Journal of Engineering Inventions* 2(7), pp.7-15.
- Bento, A.M., Viseu, T., Pêgo, J.P., Couto, L., 2021. Experimental characterization of the flow field around oblong bridge piers. *Fluids* 6(11), 370. <https://doi.org/10.3390/fluids6110370>
- Bernard, P.S., Handler, R.A., 1990. Reynolds stress and the physics of turbulent momentum transport. *Journal of Fluid Mechanics* 220, 99-124. <https://doi.org/10.1017/S0022112090003202>
- Briaud, J.L., Chen, H.C., Li, Y., Nurtjahyo, P., Wang, J., 2005. SRICOS-EFA method for contraction scour in fine-grained soils. *Journal of Geotechnical and Geoenvironmental Engineering* 131(10), 1283-1294. [https://doi.org/10.1061/\(ASCE\)1090-0241\(2005\)131:10\(1283\)](https://doi.org/10.1061/(ASCE)1090-0241(2005)131:10(1283))
- Breusers, H.N.C., Nicollet, G., Shen, H.W., 1977. Local scour around cylindrical piers. *Journal of Hydraulic Research* 15(3), 211-252. <https://doi.org/10.1080/00221687709499645>

- Bridge, J.S., Bennett, S.J., 1992. A model for the entrainment and transport of sediment grains of mixed sizes, shapes, and densities. *Water Resources Research* 28(2), 337-363. <https://doi.org/10.1029/91WR02570>
- Carnacina, I., Leonardi, N., Pagliara, S., 2019. Characteristics of flow structure around cylindrical bridge piers in pressure-flow conditions. *Water* 11(11), 2240. <https://doi.org/10.3390/w11112240>
- Cao, Z., Pender, G., Meng, J., 2006. Explicit formulation of the Shields diagram for incipient motion of sediment. *Journal of Hydraulic Engineering* 132(10), 1097-1099. [https://doi.org/10.1061/\(ASCE\)0733-9429\(2006\)132:10\(1097\)](https://doi.org/10.1061/(ASCE)0733-9429(2006)132:10(1097))
- Caroppi, G., Västilä, K., Järvelä, J., Rowiński, P.M., Giugni, M., 2019. Turbulence at water-vegetation interface in open channel flow: Experiments with natural-like plants. *Advances in Water Resources* 127, 180-191. <https://doi.org/10.1016/j.advwatres.2019.03.013>
- Cellino, M., Lemmin, U., 1999. Coherent flow structure analysis in suspension flows. *Proc. (CD-ROM) 28th IAHR Congr.*
- Clarke, B., Otto, F., Stuart-Smith, R., Harrington, L., 2022. Extreme weather impacts of climate change: an attribution perspective. *Environmental Research: Climate*, 1(1), p.012001.
- Chiew, Y.M., Melville, B.W., 1987. Local scour around bridge piers. *Journal of Hydraulic Research*, 25(1), 15-26. <https://doi.org/10.1080/00221688709499285>
- Corino, E.R., Brodkey, R.S., 1969. A visual investigation of the wall region in turbulent flow. *Journal of Fluid Mechanics* 37(1), 1-30. <https://doi.org/10.1017/S0022112069000395>
- Esfahani, F.S., Keshavarzi, A., 2011. Effect of different meander curvatures on spatial variation of coherent turbulent flow structure inside ingoing multi-bend river meanders. *Stochastic environmental research and risk assessment* 25(7), 913-928. <https://doi.org/10.1007/s00477-011-0506-4>
- Esfahani, F.S., Keshavarzi, A., 2013. Dynamic mechanism of turbulent flow in meandering channels: considerations for deflection angle. *Stochastic Environmental Research and Risk Assessment* 27(5), 1093-1114. <https://doi.org/10.1007/s00477-012-0647-0>
- Ettema, R., Melville, B.W., Barkdoll, B., 1998. Scale effect in pier-scour experiments. *Journal of Hydraulic Engineering* 124(6), pp.639-642.
- Grass, A.J. 1971. Structural features of turbulent flow over smooth and rough boundaries. *Journal of Fluid Mechanics* 50(2), 233-255. <https://doi.org/10.1017/S0022112071002556>
- Guan, D., Chiew, Y.M., Wei, M., Hsieh, S. C. 2019. Characterization of horseshoe vortex in a developing scour hole at a cylindrical bridge pier. *International Journal of Sediment Research* 34(2), 118-124. <https://doi.org/10.1016/j.ijsrc.2018.07.001>
- Huai, W.X., Zhang, J., Wang, W.J., Katul, G.G., 2019. Turbulence structure in open channel flow with partially covered artificial emergent vegetation. *Journal of Hydrology* 573, pp.180-193. <https://doi.org/10.1016/j.jhydrol.2019.03.071>
- Kabiri, F., Tabatabai, M.R.M., Shayannejad, M., 2022. Effect of vegetative bed on flow structure through a pool-riffle morphology. *Flow Measurement and Instrumentation*, 102197. <https://doi.org/10.1016/j.flowmeasinst.2022.102197>
- Kazem, M., Afzalimehr, H., Sui, J., 2021a. Characteristics of turbulence in the downstream region of a vegetation patch. *Water* 13(23), 3468. <https://doi.org/10.3390/w13233468>
- Kazem, M., Afzalimehr, H., Sui, J., 2021b. Formation of coherent flow structures beyond vegetation patches in channel. *Water* 13(20), 2812. <https://doi.org/10.3390/w13202812>
- Keshavarzi, A., Melville, B., Ball, J., 2014. Three-dimensional analysis of coherent turbulent flow structure around a single circular bridge pier. *Environmental Fluid Mechanics* 14(4), 821-847. <https://doi.org/10.1007/s10652-013-9332-1>
- Kline, S.J., Reynolds, W.C., Schraub, F.A., Runstadler, P.W., 1967. The structure of turbulent boundary layers. *Journal of Fluid Mechanics* 30(4), 741-773. <https://doi.org/10.1017/S0022112067001740>

- Kim, H., Kline, S.J., Reynolds, W.C., 1971. The production of turbulence near a smooth wall in a turbulent boundary layer. *Journal of Fluid Mechanics* 50(1), 133-160. <https://doi.org/10.1017/S0022112071002490>
- Laursen, E.M., 1963. An analysis of relief bridge scour. *Journal of the Hydraulics Division* 89(3), 93-118. <https://doi.org/10.1061/JYCEAJ.0000896>
- Liu, X., Bai, Y., 2013. Three-dimensional bursting phenomena in meander channel. *Transactions of Tianjin University* 19(1), 17-24. <https://doi.org/10.1007/s12209-013-2073-x>
- Lu, S.S., Willmarth, W.W., 1973. Measurements of the structure of the Reynolds stress in a turbulent boundary layer. *Journal of Fluid Mechanics* 60(3), 481-511. <https://doi.org/10.1017/S0022112073000315>
- Mayaud, J.R., Wiggs, G.F., Bailey, R.M., 2016. Dynamics of skimming flow in the wake of a vegetation patch. *Aeolian Research* 22, 141-151. <https://doi.org/10.1016/j.aeolia.2016.08.001>
- McGlinchey, D., 2009. *Characterisation of bulk solids*. John Wiley and Sons.
- Miyab, N.M., Fazloulou, R., Heidarpour, M., Kavian, A., Rodrigo-Comino, J., 2022. Experimental design of nature-based-solution considering the interactions between submerged vegetation and pile group on the structure of the river flow on sand beds. *Water* 14(15), 2382. <https://doi.org/10.3390/w14152382>
- Mohammadzade, N., Afzalimehr, H., Singh, V.P., 2015. Experimental investigation of influence of vegetation on flow turbulence. *International Journal of Hydraulic Engineering* 4(3), 54-69. <https://doi.org/10.5923/j.ijhe.20150403.02>
- Nortek, A.S., 2004. VECTRINO velocimeter user guide (Rev. C). *AS Nortek: Carlsbad, CA, USA*.
- Ortiz, A.C., Ashton, A., Nepf, H., 2013. Mean and turbulent velocity fields near rigid and flexible plants and the implications for deposition. *Journal of Geophysical Research: Earth Surface* 118(4), 2585-2599. <https://doi.org/10.1002/2013JF002858>
- Pickering, E., Rigas, G., Schmidt, O.T., Sipp, D., Colonius, T., 2021. Optimal eddy viscosity for resolvent-based models of coherent structures in turbulent jets. *Journal of Fluid Mechanics* 917. <https://doi.org/10.1017/jfm.2021.232>
- Pope, S.B., 2000. *Turbulent flows*. Cambridge University Press.
- Przyborowski, Ł., Łoboda, A.M., Bialik, R.J., 2019. Effect of two distinct patches of Myriophyllum species on downstream turbulence in a natural river. *Acta Geophysica* 67(3), 987-997. <https://doi.org/10.1007/s11600-019-00292-4>
- Raudkivi, A.J., Ettema, R. 1983. Clear-water scour at cylindrical piers. *Journal of Hydraulic Engineering* 109(3), 338-350. [https://doi.org/10.1061/\(ASCE\)0733-9429\(1983\)109:3\(338\)](https://doi.org/10.1061/(ASCE)0733-9429(1983)109:3(338))
- Rossi, M.J., Ares, J.O., Jobbágy, E.G., Vivoni, E.R., Vervoort, R.W., Schreiner-McGraw, A.P., Saco, P.M., 2018. Vegetation and terrain drivers of infiltration depth along a semiarid hillslope. *Science of the Total Environment* 644, 1399-1408. <https://doi.org/10.1016/j.scitotenv.2018.07.052>
- Short, F.T., Kosten, S., Morgan, P.A., Malone, S., Moore, G E., 2016. Impacts of climate change on submerged and emergent wetland plants. *Aquatic Botany* 135, 3-17. <https://doi.org/10.1016/j.aquabot.2016.06.006>
- Shahriar, A.R., Ortiz, A.C., Montoya, B.M., Gabr, M.A., 2021. Bridge Pier Scour: An overview of factors affecting the phenomenon and comparative evaluation of selected models. *Transportation Geotechnics* 28, 100549. <https://doi.org/10.1016/j.trgeo.2021.100549>
- Sterk, G., Jacobs, A. F .G., Van Boxel, J.H., 1998. The effect of turbulent flow structures on saltation sand transport in the atmospheric boundary layer. *Earth Surface Processes and Landforms: The Journal of the British Geomorphological Group* 23(10), 877-887. [https://doi.org/10.1002/\(SICI\)1096-9837\(199810\)23:10%3C877::AID-ESP905%3E3.0.CO;2-R](https://doi.org/10.1002/(SICI)1096-9837(199810)23:10%3C877::AID-ESP905%3E3.0.CO;2-R)
- Termini, D., 2015. Experimental analysis of horizontal turbulence of flow over flat and deformed beds. *Archives of Hydro-Engineering and Environmental Mechanics* 62(3-4), 77-99. <https://doi.org/10.1515/heem-2015-0021>

- Tempest, J.A., Möller, I., Spencer, T., 2015. A review of plant-flow interactions on salt marshes: The importance of vegetation structure and plant mechanical characteristics. *Wiley Interdisciplinary Reviews: Water* 2(6), 669-681.
- Vijayasree, B.A., Eldho, T.I., Mazumder, B.S., 2020. Turbulence statistics of flow causing scour around circular and oblong piers. *Journal of Hydraulic Research*, 58(4), 673-686. <https://doi.org/10.1080/00221686.2019.1661292>
- Vonkeman, J.K., Basson, G.R., 2019. Evaluation of empirical equations to predict bridge pier scour in a non-cohesive bed under clear-water conditions. *Journal of the South African Institution of Civil Engineering* 61(2), 2-20.
- Zaid, M., Yazdanfar, Z., Chowdhury, H., Alam, F., 2019. A review on the methods used to reduce the scouring effect of bridge pier. *Energy Procedia* 160, 45-50.
- Zong, L., Nepf, H. 2010. Flow and deposition in and around a finite patch of vegetation. *Geomorphology* 116(3-4), 363-372. <https://doi.org/10.1016/j.geomorph.2009.11.020>